DOI: 10.1002/cjoc.201500494

Intramolecular Charge Transfer-Enhanced BODIPY Photosensitizer in Photoinduced Electron Transfer and Its Application to Photoxidation under Mild Condition

Ruiqin Wang,[+,a] Ying Geng,[+,a] Lili Zhang,[b] Wenting Wu,*[,a] Weiyu Fan,[a] Zhongtao Li,[a] Lizhuo Wang,[a] Liying Zhan,[a] Xueyan Wu,[a] and Mingbo Wu*[,a]

[a] *State Key Laboratory of Heavy Oil Processing, School of Chemical Engineering, China University of Petroleum, Qingdao, Shandong 266580, China*

[b] *Science and Techology Bureau of Huangdao, Qingdao, Shandong 266400, China*

Photoinduced electron transfer process is a crucial step in photooxidation to obtain synthetic chemicals. However, the driving forces of electron transfer as priority in all have been rarely studied in stepwise detail. Herein, we report a series of BODIPY derivatives with an emphasis on the intramolecular charge transfer, enhancing the key step of photoinduced electron transfer process and photooxidation performances. A series of novel BODIPY photosensitizers (**B-1**—**B-5**) were prepared, wherein diethylamine amino of **B-3** as charge injection group was conjugated to the 2,6-diiodo-styryl-BODIPY, and the electron transfer impetus was enhanced 1.6 times due to its more negative redox potentials. These results were also confirmed by the DFT/TDDFT calculation. Without pure oxygen, **B-3** still can exhibit an exceptional performance in photoxidative aromatization of 1,4-DHP under mild condition. After irradiation for 28 min, the conversion rate came to 98.2%.

Keywords intramolecular charge transfer, photoinduced electron transfer , BODIPY, photosensitizers, photoxidation

Introduction

Photoinduced electron transfer (PET) process is involved in many organic photochemical reactions. It plays an important role in photooxidation and in artificial systems for the conversion of solar energy.[1-13] In PET process, the driving force for photoinduced electron transfer is crucial. Recently, much attention has been paid in compact electron donor-acceptor dyads,[14-18] but their driving forces for photoinduced electron transfer can not be easily modified by tuning redox potentials. Moreover, noble metal complexes such as ruthenium[19-21] and iridium[22,23] complexes are usually needed, which increases the cost, raises burden to environment and confines their use in milder conditions. In order to avoid the use of noble metal complexes, inorganic materials, such as TiO_2[24,25] and ZnO[26,27] have been employed as photocatalysts in photooxidation reactions. However, poor tunable ability of photoinduced electron transfer and weak visible-light harvesting ability limit their performances in photoxidation reactions.[24,28,29]

Organic photosensitizers, unlike inorganic ones, can absorb visible light and their photoredox properties can be finely modified by rational design and synthesis.[30-32] In recent years, BODIPY dyes (without noble metals) as one kind of photosensitizers, have attracted much attention.[33-39] Many researchers have focused on the modification at carbon positions of 1,3,5,7 and 8 of BODIPY.[40-42] Especially for the meso-carbon (C-8), as BODIPY dyes have inherent asymmetry in charge redistribution when they undergo $S_0 \rightarrow S_1$ transition upon excitation, C-8 owns larger charge density than other positions.[14]

Herein, we hypothesized that extending BODIPY dyes with donor and acceptor moieties at C-8 position or its opposite positions (C-3 and C-5) via intramolecular charge transfer can give different driving forces towards the electrons located at C-8. It could urge electron redistribution and finely tune redox potential. Meanwhile, it could enhance visible light harvesting ability and efficiency of photoinduced electron transfer. Zhao's[5] group and Akkaya's[6] group have reported a new 2,6-diiodo-styryl-BODIPY (**B-1**) that contains styryl groups at 3,5-C position, and they utilized this new 2,6-diiodo-BODIPY derivative to improve the reaction rate and yield of aza-Henry reaction. Based on the 2,6-diiodo-styryl-BODIPY derivative they designed,

* E-mail: wuwt@upc.edu.cn, wumb@upc.edu.cn; Tel.: 0086-0532-86984615. [+] These authors contributed equally to this work.
Received July 14, 2015; accepted September 3, 2015; published online October 28, 2015.
Supporting information for this article is available on the WWW under http://dx.doi.org/10.1002/cjoc.201500494 or from the author.

conjugating a strong donor and accepter to the derivative would facilitate its ability of photoinduced electron transfer and more creative visible-light-induced organic transformations. It is more appealing to use the series of 2,6-diiodo-styryl-BODIPY photosensitizers we designed upon light irradiation with lower intensity, which is equal to sunlight.

The oxidation product of dimethyl 1,4-dihydro-2,6-dimethylpyridine-3,5-dicarboxylate (1,4-DHP, **1a**) is of substantial significance as it is the key component in a variety of bioactive compounds, such as antihypertensive and calcium channels blocker.[43] A lot of procedures have been developed to undergo the oxidation of 1,4-DHP.[44-46] Among these, one of the very convenient approaches attracting our attention is the photoxidative aromatization method. Nevertheless, to our best knowledge, the majority of the procedures reported have to be carried in pure oxygen.[47-49] It is highly desired to design novel photosensitizers which can trigger photoxidative aromatization of 1,4-DHP under air atmosphere instead of pure oxygen, which is more economical and environmentally friendly.

In this paper, we prepared three novel photosensitizers (**B-2**, **B-3**, **B-4**) extended from 2,6-diiodo-styryl-BODIPY aforementioned and compared them with their parent compound (**B-1**) and C-8 BODIPY derivative (**B-5**), revealing the different impacts on photoinduced electron transfer process and performances in photoxidative aromatization of 1,4-DHP (**1a**) in air atmosphere.

Experimental

Measurements and materials

The NMR spectra were obtained using a 300-Bruker spectrometer, at a frequency of 400 MHz for the ^{1}H NMR. It is reported as parts per million from the internal standard, TMS. The UV-vis spectra were obtained using a Leng Guang Tech Gold Spectrumlab 54 UV-visible spectrophotometer. The fluorescence spectra were obtained using a Leng Guang Tech F97 pro spectrofluorometer. The mass spectra (MS) were determined on MALDI micro MX spectrometer. All the solvents and reagents were commercially available and of analytical reagent grade. Molecules **1** and **2** were prepared according to the reported procedures.[49-51]

Cyclic voltammetry studies

The cyclic voltammetry (CV) was performed on PARSTART 4000 instrument produced by AMETEK, in dichloromethane solution (10^{-3} mol/L) with tetrabutylammonium hexafluorophosphate (0.05 mol/L) as supporting electrolyte and glassy carbon as the working electrode and platinum wires as the counter and pseudo-reference electrode, and scan rate was 50 mV/s.

Computational methods

All calculations were performed using the Gaussian 09 software package (Gaussian, Inc.). The geometry optimizations were calculated using hybrid density functional theory (B3LYP) with the 6-31G*(d.p)/LanL2DZ basis set.

Electron spin resonance (ESR) spectroscopy

Samples were injected into quartz capillaries in darkness and illuminated in the cavity of ESR spectrometer. Photosensitizers and 5,5-dimethyl-1-pyrroline-*N*-oxide (DMPO, superoxide anion radical $O^{2\bullet-}$ scavenger) in air-saturated CH_2Cl_2 were stirred in the dark, then the solution was injected into the quartz capillaries. A diode pumped solid state (DPSS) laser (653 nm) was used for the photoirradiation of the solution in quartz capillaries for 100 s.

Molecular design and preparation of the complexes

Synthesis of B-1 **1** (50.0 mg, 0.09 mmol) and benzaldehyde (36.7 mg, 0.36 mmol) were dissolved in dry DMF (5 mL), followed by acetic acid (3 drops) and piperidine (3 drops). The mixture was put under Ar atmosphere before it was subjected to microwave irradiation (15 min, 150 ℃, 1 min pre-stirring). After removal of the solvent under reduced pressure, the mixture was purified by column chromatography (silica gel, CH_2Cl_2) to get the green section, then went through second purification (silica gel, petroleum ether∶CH_2Cl_2=2∶1, *V*/*V*), which gave a final deep purple solid. Yield 41% (28.0 mg). ^{1}H NMR (400 MHz, $CDCl_3$) δ: 8.18 (d, J=16.0 Hz, 2H), 7.73 (s, 1H), 7.69−7.66 (m, 5H), 7.55−7.52 (m, 3H), 7.44−7.41 (m, 4H), 7.37 (d, J=16.0 Hz, 2H), 7.31−7.29 (m, 2H), 1.46 (s, 6H). MALDI-HRMS calcd $[C_{33}H_{25}BF_2N_2I_2]^+$ *m*/*z* 752.0168, found *m*/*z* 752.0206.

Synthesis of B-2 Synthesis method is the same as that of **B-1**, but the benzaldehyde was replaced by 4-cyanobenzaldenhyde, finally, deep purple solid was obtained. Yield 11% (10.0 mg). ^{1}H NMR (400 MHz, $CDCl_3$) δ: 8.17 (d, J=12.0 Hz, 1H), 8.03 (d, J=8.0 Hz, 1H), 7.88 (d, J=8.0 Hz, 1H), 7.79 (s, 1H), 7.75−7.73 (m, 7H), 7.60 (d, J=4.0 Hz, 2H), 7.56−7.54 (m, 2H), 7.33 (d, J=8.0 Hz, 2H), 1.50 (s, 6H). MALDI-HRMS calcd $[C_{35}H_{23}BF_2N_4I_2]^+$ *m*/*z* 802.0073, found *m*/*z* 802.0107.

Synthesis of B-3 Synthesis method is the same as that of **B-1**, but the benzaldehyde was replaced by 4-diethylamino benzaldehyde, finally, deep purple solid was obtained. Yield 22% (15.0 mg). ^{1}H NMR (400 MHz, $CDCl_3$) δ: 8.25−8.21 (d, J=16 Hz, 1H), 7.56−7.28 (m, 6H), 6.70−6.68 (d, J=8 Hz, 2H), 3.46−3.42 (m, 4H), 1.58 (s, 2H), 1.45 (s, 3H), 1.39 (s, 3H), 1.27−1.21 (m, 9H). MALDI-HRMS calcd $[C_{30}H_{30}BF_2N_3I_2]^+$ *m*/*z* 735.0590, found *m*/*z* 735.0490.

Synthesis of B-4 Synthesis method is the same as that of **B-3**, but **1** was replaced by **2**, finally, deep purple solid was obtained. Yield: 56% (20.0 mg). ^{1}H NMR (400 MHz, $CDCl_3$) δ: 8.55 (d, J=8 Hz, 2H), 8.43 (d, J=8 Hz, 1H), 7.69−7.61 (m, 5H), 6.82 (d, J=8 Hz, 2H), 5.44 (s, 1H), 3.59−3.54 (m, 4H), 2.81 (s, 3H),

CHINESE JOURNAL OF CHEMISTRY

Scheme 1 Synthesis strategy of 2,6-diiodo-styryl-BODIPY derivatives

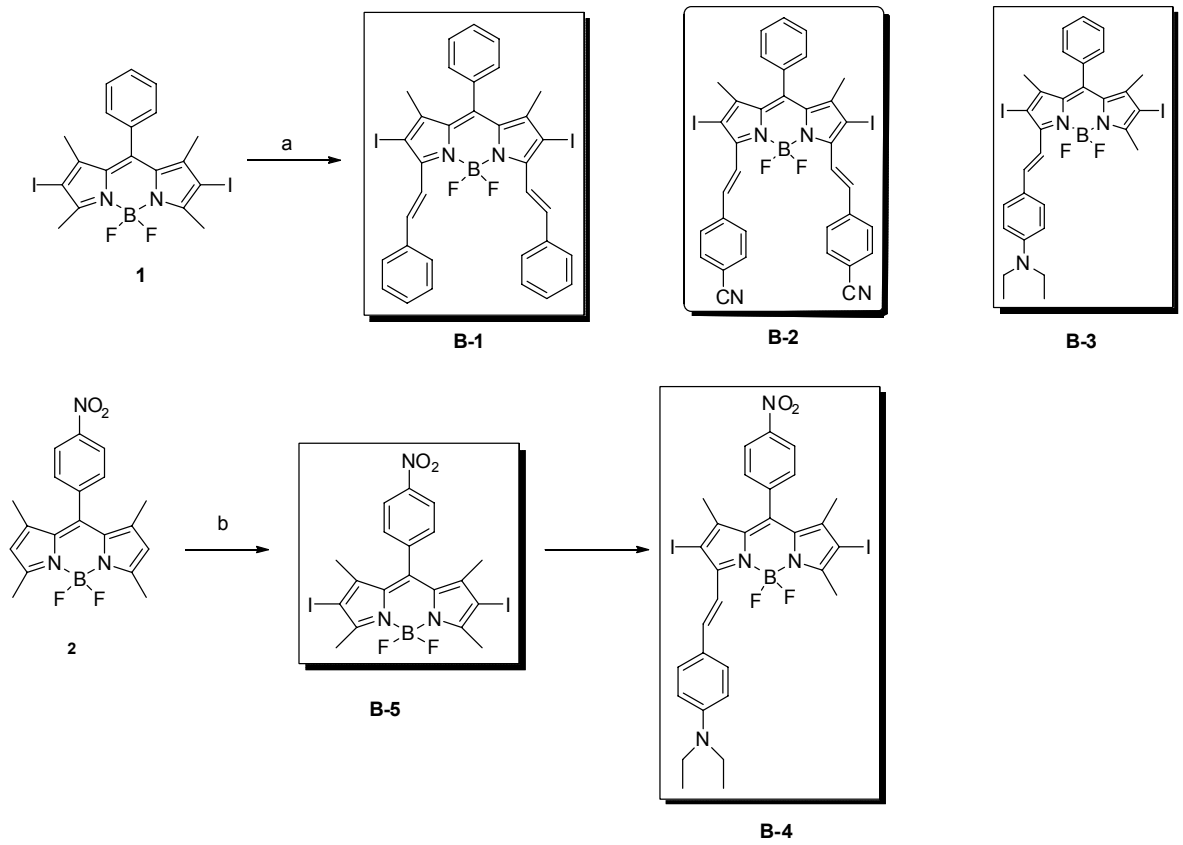

(a) Piperidine, AcOH, DMF, microwave, 150 °C; (b) *N*-iodosuccinimide, dichloromethane, room temperature

1.69 (s, 2H), 1.39 (s, 3H), 1.39－1.33 (m, 6H). MALDI-HRMS calcd $[C_{30}H_{29}BF_2N_4I_2O_2]^+$ *m*/*z* 780.0441, found *m*/*z* 780.0397.

Synthesis of B-5 **2** (300.0 mg, 0.8 mmol) and *N*-iodosuccinimide (720.0 mg, 3.2 mmol) were dissolved in 80 mL CH_2Cl_2. After stirring for 12 h at room temperature, the solvent was removed under reduced pressure, the mixture was purified by column chromatography (silica gel, petroleum ether∶CH_2Cl_2＝2∶1, *V*/*V*). Yield: 90% (447.0 mg). ^{1}H NMR (400 MHz, $CDCl_3$) δ: 8.44 (d, *J*＝8 Hz, 2H), 7.54 (d, *J*＝8 Hz, 2H), 2.67 (s, 6H), 1.38 (s, 6H). MALDI-HRMS calcd $[C_{19}H_{16}BF_2N_3I_2O_2]^+$ *m*/*z* 620.9393, found *m*/*z* 620.9366.

General procedure of photoxidative aromatization of 1, 4-DHP

150 μL 1,4-DHP (**1a**, dissolved in CH_2Cl_2, 3×10^{-2} mol/L) and 10 μL photosensitizer (dissolved in CH_2Cl_2, 1.0×10^{-3} mol/L) were injected into a two-neck flask containing 10 mL CH_2Cl_2. The reaction was conducted under air atmosphere, and the solution was irradiated at r.t. with a 30 W xenon lamp by cutting off the light of ＜385 nm. The irradiation intensity was 25 mW/cm^2. UV-vis absorption spectra were recorded at intervals of 1－2 min. The consumption of **1a** and yield of its aromatization product (**1b**) were recorded by UV absorption. The ^{1}H NMR and MS results of the aromatization product (**1b**) were collected in Supporting Information. ^{1}H NMR (400 MHz, $CDCl_3$) δ: 8.68 (s, 1H), 4.42－4.38 (m, 4H), 2.85 (s, 6H), 1.43－1.40 (m, 6H). MALDI-HRMS calcd $[C_{13}H_{17}NO_4]^-$ Na^+ *m*/*z* 274.1055, found *m*/*z* 274.1060.

The spectra of compounds **1** and **2** have been reported.[53,54]

Results and Discussion

Electrochemical studies

In order to determine the electron transfer direction and electron transfer ability of the photosensitizers, the electrochemical properties of the photosensitizers[55,56] were studied as shown in Table 1.

Among all the reversible reduction potentials, the onset potential is attributed to the formation of stable BODIPY core anions, which is located at −0.5－−0.77 V. As for **B-2** and **B-4**, the second reversible reduction refers to the formation of CN substitute (−1.28 V vs. NHE) and NO_2 substitute (−1.02 V vs. NHE), respectively. The reversible oxidations of photosensitizers above 1.25 V vs. NHE in the Table 1 are assigned to BODIPY core. The onset reversible oxidations of **B-3** (0.87 V vs. NHE) and **B-4** (0.94 V vs. NHE) are assigned to diethylamino groups, which make **B-3** and **B-4** release electrons more easily from the photosensitizers to other substrate molecules in photocatalytic organic reactions. Due to introducing $-NO_2$ into **B-4**, the onset oxidation of **B-3** (0.87 V vs. NHE) is more negative than that of **B-4** (0.94 V vs. NHE), which means the electron transfer impetus of **B-3**

Table 1 Electrochemical data and the calculated HOMO, LUMO and ΔG^{o} values

Compd.	E_{ox}[a]/V	E_{red}[a]/V	HOMO[b]/eV	LUMO[b]/eV	$\Delta G_1{}^{o}$ [c]/(kJ•mol^{-1})	$\Delta G_2{}^{o}$ [d]/(kJ•mol^{-1})
B-1	1.32	−0.50	−6.07	−4.25	−1.51	−0.03
B-2	1.25	−0.63/−1.28	−6.00	−4.12	−1.38	−0.07
B-3	0.87/1.28	−1.17	−5.62	−3.58	−0.84	−0.42
B-4	0.94/1.35	−0.67/−1.02	−5.69	−4.08	−1.34	−0.29
B-5	1.58	−0.77/−1.04	−6.33	−3.98	−0.53	−0.20

[a] Redox potential (vs. NHE, CH_2Cl_2). [b] HOMO and LUMO energy values were calculated based on the equations: E_{HOMO}= −($E_{[onset, ox vs. NHE]}$ +4.75) (eV), E_{LUMO}=−($E_{[onset, red vs. NHE]}$ +4.75) (eV).[52] [c] The thermodynamic driving force for photoinduced electron transfer was calculated based on the Rehm-Weller Equation. $\Delta G_1{}^{o}$ stands for the thermodynamic driving force for electron transfer process from 1,4-DHP to photosensitizers. [d] $\Delta G_2{}^{o}$ stands for the thermodynamic driving force for electron transfer process from photosensitizers to O_2.

was enhanced 1.6 times compared with that of the other photosensitizers, indicating that **B-3** owns the strongest electron-donating ability among the designed photosensitizers. The photosensitizers act as either electron acceptor (reductive quenching) or electron donor (oxidative quenching) in the first step of the photocatalytic cycles, then play an opposite role to recover to the original state in the next step. Therefore, the photoredox properties of photosensitizers (both electron-donating and electron-accepting abilities) play an important role in the electron transfer process of the photocatalytic organic reactions. The contribution of different groups of photosensitizers to the electron transfer was discussed in detail.

Absorption and emission abilities of the photosensitizers

UV-vis absorption spectra of the complexes were studied in dichloromethane (Figure 1).[57] Due to the large extended conjugation of styryl in BODIPY, **B-1**, **B-2**, **B-3** and **B-4** show obvious red shifts in comparision with **B-5**. Interestingly, the UV-vis absorptions of **B-1** and **B-2** have dual intense absorption at around 350 and 640 nm, respectively, indicating that there is no apparent intramolecular charge transfer effect (ICT). Conversely, **B-3** and **B-4** show single intense absorption at

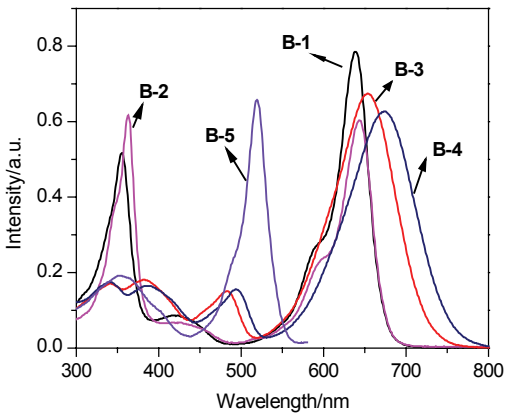

Figure 1 UV-Vis absorption spectra of **B-1**, **B-2**, **B-3**, **B-4** and **B-5** in dichloromethane (1.0×10^{-5} mol/L, 20 ℃).

656 and 675 nm, respectively. For example, **B-4** with diethyl amino substituent at C-3 and nitrobenzol substituent at C-8 shows an enhanced ICT effect, resulting in single intense absorption at 675 nm and a more than 150 nm red shifts compared to **B-5**. It is worth mentioning that all the photosensitizers we designed (**B-2**, **B-3** and **B-4**) exhibit intense absorption with molar extinction coefficients of around 6×10^{4} mol^{-1}•L•cm^{-1} in red region. The intense absorption ability is believed to benefit the light harvest in the photocatalytic organic reactions.

The fluorescence spectra of the photosensitizers we prepared were examined in various solvents with different polarities and then compared with that of **B-1** (see Figure 2a). For free substituted photosensitizer **B-1**, the emission wavelength is at 665 nm in toluene and 666 nm in the mixed solvent of DMF and H_2O. **B-2** with CN substitute at C-3, 5 positions (Figure 2b) and **B-5** with NO_2 at C-8 position (Figure S13) show similar phenomena: with increasing solvent polarity, there is no distinct red shift, indicating that there is no evident intramolecular electron transfer. Conversely, for **B-3** with diethyl amino substitute at C-3 position, its emission wavelength shows about 77 nm red shift, while its emission intensity in CH_2Cl_2 is quenched above 80% in comparison with that in toluene (Figure 2c). For **B-4** with NO_2 at the opposition of diethyl amino substitute (Figure 2d), its emission wavelength shows a more red shift, while its emission intensity is almost completely quenched in CH_2Cl_2 (Table S1). These phenomena indicate that the ability of intramolecular electron transfer for **B-3** and **B-4** is enhanced. The absorption spectral change of BODIPY (1×10^{-5}) in CH_2Cl_2 without 1,4-DHP is shown in Figure S14. The fluorescence quantum yields of **B-1**, **B-2**, **B-3**, **B-4** and **B-5** in CH_2Cl_2 are shown in Table S2.

DFT calculations: intramolecular electron transfer

DFT calculations for the photosensitizers extended on the designed BODIPY, at the B3LYP/6-31G (d, p) level of theory, support directional movement of charge on excitation, especially for **B-3** and **B-4**.

The calculated electron distributions and energy lev-

CHINESE JOURNAL OF CHEMISTRY

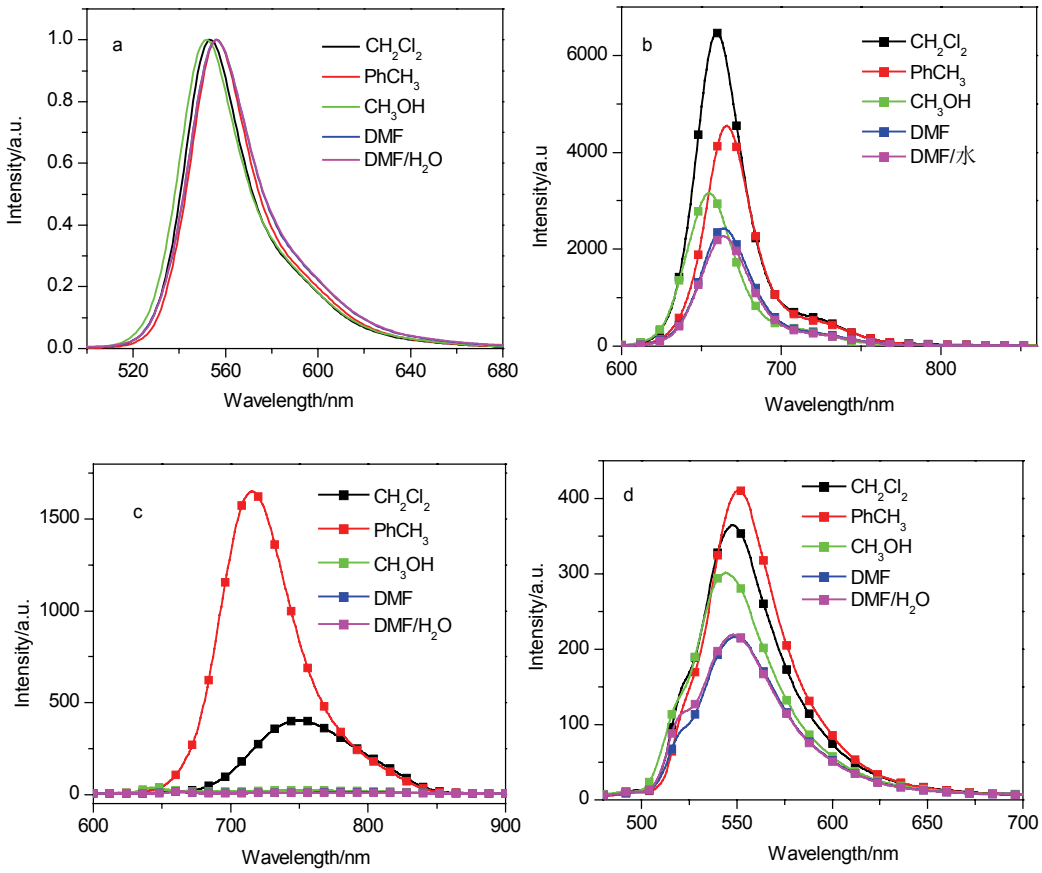

Figure 2 Fluorescence spectra of (a) **B-1**, (b) **B-2**, (c) **B-3** and (d) **B-4** in different solvents (CH_2Cl_2, toluene, methanol, DMF, DMF/H_2O V/V=5∶1). (1.0×10^{-5} mol/L, 20 ℃).

els of HOMO and LUMO of the photosensitizers extended on BODIPY we designed are shown in Figure 3 and Figure S15. For all the prepared molecules, the HOMO isosurfaces are mainly delocalized over the π framework of the BODIPY and the styryl groups, whereas LUMO isosurfaces show the big differences among the molecules. The LUMO electron density of **B-3** reveals a trend of electron transfer from the styryl substituents to the BODIPY moiety upon a vertical excitation of the π→π* type, which indicates the preference of electron transfer in photocatalytic reactions. But for **B-4**, as nitrobenzol substitute grabs electrons partially, it becomes harder to release electrons when interacts with substrate molecules in reactions, although it shows the lowest HOMO-LUMO gap (2.09 eV). However, for **B-2** and **B-5**, there is no significant change between HOMO and LUMO electron density, which indicates poor electron-transfer abilities of **B-2** and **B-5** on excitation. Moreover, the HOMO-LUMO gap of **B-5** is much larger, which indicates a less reactive character of **B-5**. All in all, the electron transfer differences are in consistent with the CV results aforementioned. Although the calculated energy levels are a little higher than the ones determined experimentally, the trends in the band gaps are in good agreement with the ones obtained by CV analyses.

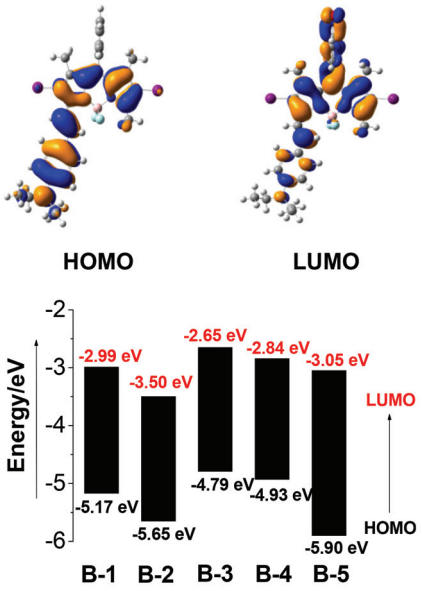

Figure 3 Electron density maps of the frontier molecular orbitals of **B-3** and calculated energy levels (HOMO and LUMO) of all the photosensitizers.

Photoxidation of 1,4-DHP under air atmosphere

In order to compare the contribution of different groups of photosensitizers to the electron transfer, the photoxidation of 1,4-DHP was catalyzed by prepared

photosensitizers, which was irradiated under air atmosphere instead of pure oxygen atmosphere. The photocatalytic processes were monitored by UV-Vis absorption spectrum, recording the absorption decrease at 350 nm for **1a** and the absorption increase at 280 nm for the product (**1b**).[47]

The changes of UV curves and the rate of the reactions are demonstrated in Figures 4 and 5, respectively. As the performance of the photocatalysts differs greatly with each other (Table 2), the reaction time was set to 34 min. After irradiation for 28 min, the yield of **B-3** comes to 98.2%, the next is **B-1** (95.5%), followed by **B-2** (94.3%), **B-5** (69.7%) and **B-4** (11.9%). The reactions photocatalyzed by **B-1** and **B-2** stopped at 18 min (Figure S16).

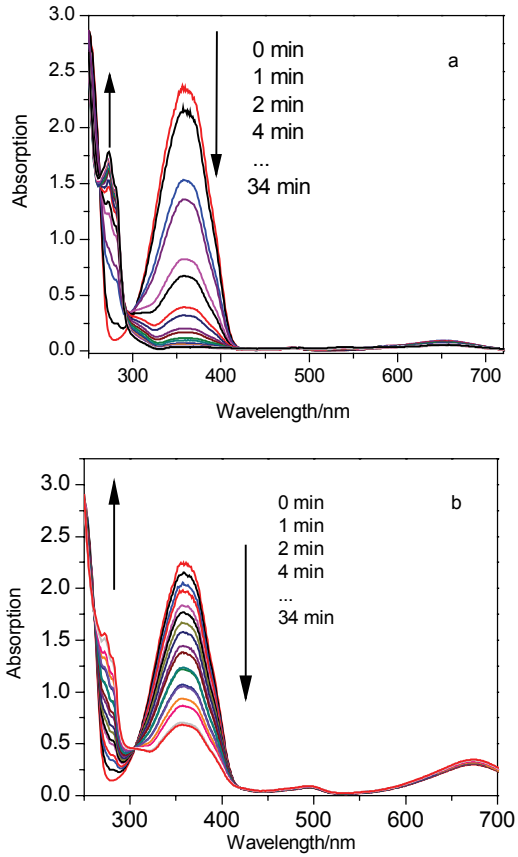

Figure 4 UV-Vis absorption changes of **1a** (4.5×10^{-3} mol/L) in dichloromethane (10 mL) upon irradiation at $\lambda>420$ nm, catalyzed by photosensitizers of (a) **B-3**, (b) **B-4** (1.0×10^{-6} mol/L). Arrows denote the evolution of the absorption spectra with increasing time. Irradiation time was respectively 0, 1, 2, 4, 8, 10, ⋯, 34 min.

The mechanism for photoxidative aromatization of **1a** catalyzed by **B-3** is proposed in Scheme 2. At first, **B-3** is photoexcited to singlet excited state, and photoinduced electron transfer (PET) from **1a** to **B-3** (electron acceptor) produces highly reactive **1a** cation radical which is preferable to release H^+ subsequently. Then, electron transfer process from **1a** radical to O_2 results in the production of final aromatization product (**1b**) and

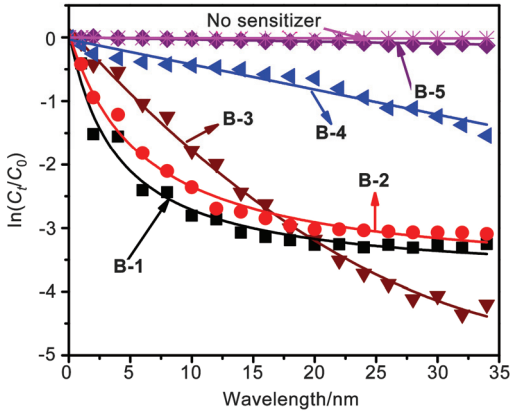

Figure 5 Plots of $\ln(C_t/C_0)$ vs. irradiation time (min) for the photooxidative aromatization of **1a**, concentration was determined by the UV-Vis absorption changes at 360 nm.

Table 2 Photoxidative aromatization of 1,4-DHP catalyzed by the photosensitizers we prepared

Entry	Photosensitizer[a]	Solvent	t^b/min	Yield[c]/%	TON[d]	TOF[e]/min^{-1}
1	—	CH_2Cl_2	34	0.51	—	—
2	**B-1**	CH_2Cl_2	18	95.5	429.8	12.6
3	**B-2**	CH_2Cl_2	18	94.3	424.4	12.4
4	**B-3**	CH_2Cl_2	28	98.2	441.9	13.0
5	**B-4**	CH_2Cl_2	34	69.7	313.7	9.2
6	**B-5**	CH_2Cl_2	34	11.9	53.6	1.6

[a] $C=4.5\times10^{-6}$ mol/L. [b] Judged by curves of $\ln(C_t/C_0)$ vs. t (min) (see Figure 5). [c] Yields were determined by the UV-Vis absorption changes. [d] Turnover number, calculated by the molar ratio of the production to the catalysts. [e] Turnover frequency.

reactive oxygen radical. At last, reactive oxygen radical grabs electron from **B-3** radical (electron donor), recovering the photosensitizer, and at the same time superoxide anion radical is produced.

In order to trap the possible $O^{2\bullet-}$ and further to confirm the mechanism, electron spin resonance (ESR) spectroscopy was employed, with the 5,5-dimethyl-1-pyrroline-*N*-oxide (DMPO) as scavenger for $O^{2\bullet-}$. Firstly, the mixture of **B-3** and DMPO in aerated CH_2Cl_2 was analyzed by ESR spectroscopy. No signal was detected. This result indicates that **B-3** alone does not produce $O^{2\bullet-}$ (Figure S17a). Next, **1a** and **B-3** were mixed in aerated CH_2Cl_2 (Figure S17b). The signal due to DMPO−$O^{2\bullet-}$ was detected, indicating that $O^{2\bullet-}$ was produced with **B-3** (electron acceptor) in the presence of **1a** (electron donor), that is, the electron transfer from substrate to the photosensitizer occurs, followed by the electron transfer from photosensitizer to $O^{2\bullet}$. H_2O_2 was also detected by using KI/CH_3COOH. A brown colour was observed when mixing the reaction system (already irradiated for 30 min) with KI/CH_3COOH (Figure S18), which indicates $O^{2\bullet-}$ was really involved in the photoxidaive aromatization of 1,4-DHP catalyzed by the pho-

tosensitizers we designed.

Scheme 2 Procedure of photoxidative aromatization of **1a** (1,4-DHP) catalyzed by **B-3**

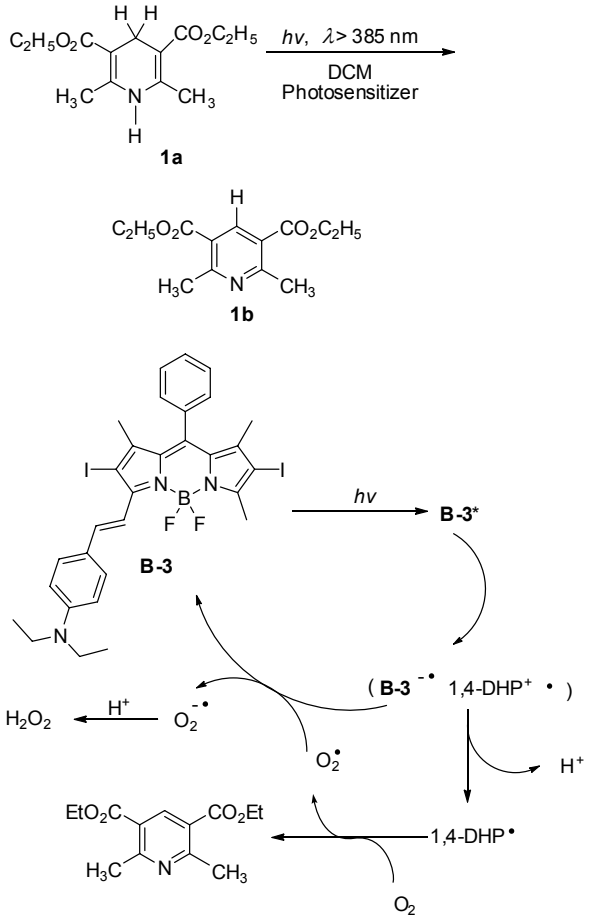

B-3 alone and **B-3** with 1,4-DHP were measured with ESR spectra after adding 2,2,6,6-tetramethyl-piperidine (TEMP). These results suggest the existence of $^1O_2$ (Figure S17c—d). However, there are no obvious intensity changes, indicating that $^1O_2$ is not involved into the first step of the catalytic cycle.

Based on the confirmed mechanism, the electron transfer processes (photocatalyst*→1,4-DHP, photocatalyst$^{\bullet-}$→$O^{2\bullet}$) are crucial for the photooxidation reaction. The thermodynamic driving force (ΔG_1^o, ΔG_2^o, see Table 1) of each step calculated by the Rehm-Weller equation[58] was used to quantify the photooxidative reaction of 1,4-DHP. Firstly, the photoexcited sensitizer grabs one electron from 1,4-DHP, which is easy for all photosensitizers. Although the ΔG_1^o of **B-3** is much higher than those of **B-1**, **B-2** and **B-4**, **B-3** shows the best catalytic performance. So the reductive quenching ability of photosensitizer is not crucial in the whole reaction, and the electron-accepting ability of **B-3** seems enough in the first step. In the second step, the photosensitizer anion recovers to the original state via donating its electron to oxygen. It is noteworthy that distinctive differences of ΔG_2^o occur: **B-3** owns the most negative ΔG_2^o (−0.42), whereas **B-1** and **B-2** show little tendancy to react with oxygen. It is believed that the oxidative quenching abiliy of photosensitizer is crucial for acquiring a satisfactory catalytic performance in photooxidizing 1,4-DHP. As a result of charge injection of diethyl amino, **B-3** shows the highest activity in the photoxidation of 1,4-DHP than others under air atmosphere (Figure 5a). It is noted that the reaction time in this paper is 28 min, even less than half of the time that usually needed in current photocatalysts for the photoxidaive aromatization of 1,4-DHP.[41,43]

Conclusions

We have successfully designed and synthesized a series of 3,5-styryl-BODIPY photosensitizers. The resulting photosensitizers exhibit strong absorptions in red region (around 6×10^4 L•mol^{-1}•cm^{-1}). Moreover, conjugating diethylamino to the 2,6-diiodo-styryl-BODIPY (**B-3**) can enhance the photoinduced electron transfer process by 1.6 times due to the more negative redox potential (0.87 V vs. NHE), guaranteeing a much better catalysis effect in photocatalytic area than 2,6-diiodo-styryl-BODIPY (**B-1**) in literature. **B-3** shows excellent activity in the photoxidative aromatization of 1,4-DHP even under air atmosphere. The conversion ratio of 1,4-DHP can reach 98% within 0.5 h, even less than half of the time usually needed in pure oxygen, indicating the good application future of synthesized 3,5-styryl-BODIPY photosensitizers in the photoxidative reactions.

Acknowledgement

We thank the support of National Natural Science Foundation of China (Grant 21302224, 51172285, 21176259, 51303212, 51303202), China Postdoctoral Science Foundation (2014M560590, 2015T80758), Fundamental Research Funds for the Central Universities (15CX05010A), Shandong Provincial Natural Science Foundation (ZR2013BQ028, ZR2013EMQ013), Project of Science and Technology Program for Basic Research of Qingdao (14-2-4-47-jch) and the State Key Laboratory of Fine Chemicals (KF1203).

References

[1] Hirakawa, T.; Yawata, K.; Nosaka, Y. *Appl. Catal. A-Gen.* **2007**, *1*, 105.
[2] Nilushika, D.; Awad, M.-I.; Saleh, M.-M.; Okajima, T.; Mao, L.; Ohsaka, T. *Chem. Commun.* **2015**, *16*, 3343.
[3] Wada, A.; Jitsukawa, K.; Masuda, H. *Angew. Chem., Int. Ed.* **2013**, *47*, 125.
[4] Hintz, S.; Mattay, J.; Eldik, R.; Fu, W. *Eur. J. Org. Chem.* **1998**, *8*, 1583.
[5] Huang, L.; Zhao, J.-Z. *RSC Adv.* **2013**, *45*, 23377.
[6] Bozdemir, O.-A.; Guliyev, R.; Buyukcakir, O.; Selcuk, S.; Kolemen, S.; Gulseren, G.; Nalbantoglu, T.; Boyaci, H.; Akkaya, E.-U. *J. Am. Chem. Soc.* **2010**, *132*, 8029.
[7] Hirakawa, T.; Nosaka, Y. *J. Phys. Chem. C* **2008**, *40*, 15818.
[8] Fang, X.; Liu, Y.-C.; Li, C. *J. Org. Chem.* **2007**, *22*, 8608.

[9] Barata-Vallejo, S.; Flesia, M.-M.; Lantaño, B.; Argüello, J.-E.; Peñéñory, A.-B.; Postigo, A. *Eur*. *J*. *Org*. *Chem*. **2013**, *5*, 998.
[10] Fukuzumi, S.; Yamada, Y.; Suenobu, T.; Ohkubo, K.; Kotani, H. *Energ*. *Environ*. *Sci*. **2011**, *8*, 2754.
[11] Harriman, A.; Sauvage, J.-P.-A. *Chem*. *Soc*. *Rev*. **1996**, *1*, 41.
[12] Ma, X.; Azeem, E.-A.; Liu, X.; Cheng, Y.; Zhu, C. *J*. *Mater*. *Chem*. *C* **2014**, *6*, 1076.
[13] Guldi, D.-M.; Gouloumis, A.; Vázquez, P.; Torres, T. *Chem*. *Commun*. **2002**, 2056.
[14] Erten, E.-S.; Yilmaz, M.-D.; Icli, B.; Dede, Y.; Icli, S.; Akkaya, E.-U. *Org*. *Lett*. **2008**, *15*, 3299.
[15] Pelado, B.; Abou-Chahine, F.; Calbo, J.; Caballero, R.; Cruz, P.-D.-L.; Junquera-Hernández, J.-M.; Enrique, O.; Nikolai, V.-T.; Langa, F. *Chem*. *Eur*. *J*. **2015**, *15*, 5814.
[16] Nascimento, S.; Fedorov, A.; Brites, M.-J.; Berberan-Santos, M.-N. *Dyes Pigments* **2015**, *114*, 158.
[17] Pfattner, R.; Pavlica, E.; Jaggi, M.; Liu, S.-X.; Decurtins, S.; Bratina, G.; Veciana, J.; Mas-Torrent, M.; Rovira, C. *J*. *Mater*. *Chem*. *C* **2013**, *25*, 3985.
[18] Ley, D.; Guzman, C.-X.; Adolfsson, K.-H.; Scott, A.-M.; Brauschweig, A.-B. *J*. *Am*. *Chem*. *Soc*. **2014**, *22*, 7809.
[19] Joachim, K.; Robert, S.; Maria, W.; Ulrich, S.-S.; Benjamin, D.; Michael, J. *J*. *Phys*. *Chem*. *C* **2015**, *9*, 4742.
[20] Gunderson, V.-L.; Krieg, E.; Vagnini, M.-T.; Iron, M.-A.; Rybtchinski, B.; Wasielewski, M.-R. *J*. *Phys*. *Chem*. *B* **2011**, *23*, 7533.
[21] Sato, T.; Nozawa, S.; Tomita, A.; Hoshino, M.; Koshihara, S.-Y.; Fujii, H. *J*. *Phys*. *Chem*. *C* **2012**, *27*, 14232.
[22] Liu, S.-J.; Lin, W.-P.; Yi, M.-D.; Xu, W.-J.; Tang, C.; Zhao, Q.; Ye, S.-H.; Liu, X.-M.; Huang, W. *J*. *Mater*. *Chem*. **2012**, *43*, 22964.
[23] Wenger, O.-S. *Coordin*. *Chem*. *Rev*. **2015**, *282*, 150.
[24] (a) Lin, X.-H.; Li, S.-F.-Y. *Appl*. *Catal*. *B Environ*. **2015**, *170*, 263; (b) Guillard, C.; Disdier, J.; Herrmann, J.-M.; Lehaut, C.; Chopin, T.; Malato, S.; Blanco, J. *Catal*. *Today* **1999**, *2*, 217.
[25] (a) Gaya, U.-I.; Abdullah, A.-H. *J*. *Photochem*. *Photobiol*. *C* **2008**, *1*, 1; (b) Li, Y.; Wen, B.; Yu, C.; Chen, C.; Ji, H.; Ma, W.; Zhao, J. *Chem*. *Eur*. *J*. **2012**, *1*, 2030.
[26] Tian, C.; Zhang, Q.; Wu, A.; Jiang, M.; Liang, Z.; Jiang, B.; Fu, H. *Chem*. *Commun*. **2012**, *23*, 2858.
[27] Choina, J.; Bagabas, A.; Fischer, C.; Flechsig, G.-U.; Kosslick, H.; Alshammari, A.; Schulz, A. *Catal*. *Today* **2015**, *241*, 47.
[28] (a) Weber, A.-S.; Grady, A.-M.; Koodali, R.-T. *Catal*. *Sci*. *Technol*. **2012**, *4*, 683; (b) Tada, H.; Kiyonaga, T.; Naya, S. *Chem*. *Soc*. *Rev*. **2009**, *7*, 1849.
[29] (a) Wang, Y.; Bai, X.; Pan, C.; He, J.; Zhu, Y. *J*. *Mater*. *Chem*. **2012**, *23*, 11568; (b) Fu, H.; Zhang, L.; Yao, W.; Zhu, Y. *Appl*. *Catal*. *B* **2006**, *1*, 100.
[30] Ravelli, D.; Dondi, D.; Fagnoni, M.; Albini, A. *Chem*. *Soc*. *Rev*. **2009**, *7*, 1999.
[31] Marin, M.-L.; Santos-Juanes, L.; Arques, A.; Amat, A.-M.; Miranda, M.-A. *Chem*. *Rev*. **2012**, *3*, 1710.
[32] Erbas-Cakmak, S.; Cakmak, F.-P.; Topel, S.-D.; Uyar, T.-B.; Akkaya, E.-U. *Chem*. *Commun*. **2015**, *61*, 12258.
[33] Zhou, Y.; Zhou, Z.; Li, Y.; Yang, W. *Catal*. *Commun*. **2015**, *64*, 96.
[34] Kamkaew, A.; Lim, S.-H.; Lee, H.-B.; Kiew, L.-V.; Chung, L.-Y.; Burgess, K. *Chem*. *Soc*. *Rev*. **2013**, *1*, 77
[35] Caruso, E.; Banfi, S.; Barbieri, P.; Leva, B.; Orlandi, V.-T. *J*. *Photochem*. *Photobiol*. *B* **2012**, *114*, 44.
[36] Banfi, S.; Caruso, E.; Zaza, S.; Mancini, M.; Marzia, B.-G.; Monti, E. *J*. *Photochem*. *Photobiol*. *B* **2012**, *114*, 52.
[37] (a) Orlandi, V.-T.; Rybtke, M.; Caruso, E.; Banfi, S.; Tolker, N.-T.; Barbieri, P. *Biofouling* **2014**, *30*, 883; (b) Banfi, S.; Nasini, G.; Zaza, S.; Caruso, E. *Tetrahedron* **2013**, *69*, 4845.

(Zhao, X.)

